Available online at www.sciencedirect.com
ScienceDirect
International Journal of Pharmaceutics 342 (2007) 124–136
INTERNATIONAL JOURNAL OF PHARMACEUTICS
www.elsevier.com/locate/ijpharm

# Colon-specific delivery of 5-aminosalicylic acid from chitosan-Ca-alginate microparticles

K. Mladenovska [a,*], R.S. Raicki [a,1], E.I. Janevik [b,2], T. Ristoski [c,3], M.J. Pavlova [b,2], Z. Kavrakovski [a,1], M.G. Dodov [a,1], K. Goracinova [a,1]

[a] *Ss. Cyril and Methodious University, Faculty of Pharmacy, Vodnjanska 17, 1000 Skopje, Macedonia*
[b] *Ss. Cyril and Methodious University, Faculty of Medicine, Vodnjanska 17, 1000 Skopje, Macedonia*
[c] *Ss. Cyril and Methodious University, Faculty of Veterinary medicine, Lazar Pop Trajkov, 5-7, 1000 Skopje, Macedonia*

Received 10 January 2007; received in revised form 4 May 2007; accepted 4 May 2007
Available online 21 May 2007

**Abstract**

Chitosan-Ca-alginate microparticles for colon-specific delivery and controlled release of 5-aminosalicylic acid after peroral administration were prepared using spray drying method followed by ionotropic gelation/polyelectrolyte complexation. Physicochemical characterization pointed to the negatively charged particles with spherical morphology having a mean diameter less than 9 μm. Chitosan was localized dominantly in the particle wall, while for alginate, a homogeneous distribution throughout the particles was observed. $^{1}$H NMR, FTIR, X-ray and DSC studies indicated molecularly dispersed drug within the particles with preserved stability during microencapsulation and in simulated *in vivo* drug release conditions. *In vitro* drug release studies carried out in simulated *in vivo* conditions in respect to pH, enzymatic and salt content confirmed the potential of the particles to release the drug in a controlled manner. The diffusional exponents according to the general exponential release equation indicated anomalous (non-Fickian) transport in 5-ASA release controlled by a polymer relaxation, erosion and degradation. Biodistribution studies of [$^{131}$I]-5-ASA loaded chitosan-Ca-alginate microparticles, carried out within 2 days after peroral administration to Wistar male rats in which TNBS colitis was induced, confirmed the dominant localization of 5-ASA in the colon with low systemic bioavailability.


*Keywords:* Chitosan-Ca-alginate microparticles; 5-Aminosalicylic acid; Inflammatory bowel diseases; Controlled release; Colon delivery

## 1. Introduction

5-Aminosalicylic acid (5-ASA) is an anti-inflammatory drug commonly used in the treatment of Crohn's disease and ulcerative colitis, which may provide protection against the development of colorectal cancer in patients suffering from inflammatory bowel diseases (IBD) (Bernstein et al., 2002; Kuang et al., 2002). It appears that many of the effects of 5-ASA can be explained by inhibition of activation of nuclear Factor-κB (NF-κB), which is a central transcription regulatory factor involved in mediating the initiation and perpetuation of inflammatory processes (Bantel et al., 2000; MacDermott and Richard, 2000; D'Acquisto et al., 2002). 5-ASA was demonstrated to inhibit TNF-α stimulated NF-κB activation, NF-κB nuclear translocation and degradation of inhibitory κBα (Kaiser et al., 1999; Verziji and van Bodegraven, 2003).

Activated NF-κB has been detected in macrophages and epithelial cells of colonic biopsies from Crohn's disease and ulcerative colitis patients (Rogler et al., 1998; Schreiber et al., 1998; Schreiber, 1999; Wahl et al., 1998). In this respect, efficacy of 5-ASA correlates with tissue delivery and therefore factors, such as intestinal metabolism and elimination that affect tissue delivery may be important in determining its efficacy (Zhou et al., 1999a). 5-ASA is rapidly absorbed from the small intestine and there is a little localization of 5-ASA in the colon relative to the small intestine (Zhou et al., 1999b). Oral administration is limited also due to the serious adverse effects, such as hepatitis, blood dyscrasias, pancreatitis, pleuropericarditis and interstitial

* Corresponding author. Tel.: +389 2 3126 032; fax: +389 2 3123 054.
*E-mail address:* krml@ff.ukim.edu.mk (K. Mladenovska).
[1] Tel.: +389 2 3126 032; fax: +389 2 123 054.
[2] Tel.: +389 2 3112 831; fax: +389 2 3147 203.
[3] Tel.: +389 2 3240 700; fax: +389 2 3114 619.

0378-5173/$ – see front matter © 2007 Elsevier B.V. All rights reserved.
doi:10.1016/j.ijpharm.2007.05.028

nephritis associated with 5-ASA therapy (Loftus et al., 2004).

Three methods have been widely used for targeting of 5-ASA to the colon: a pro-drug concept, enteric coating and/or prolonged release of the drug through semipermeable membrane (Prakash and Markharm, 1999; Clemett and Markham, 2000; Loftus et al., 2004). Controlled release preparations are specifically designed to minimize systemic absorption and to achieve optimum delivery of the biologically active 5-ASA moiety to the distal small intestine and the colon. Thus, relatively high concentrations of free 5-ASA can be achieved in the intestinal lumen without producing systemic exposure and subsequent toxicity. This type of target tissue selectivity is a desirable feature for chemopreventive agents and is a significant advantage when considering drug delivery methods to the mucosal surface of the gut.

For these requirements, we have designed a new microparticulate system consisting of chitosan-Ca-alginate matrix in which 5-ASA was dispersed. The use of chitosan provides great promise due to its mucoadhesive properties and non-solubility at pH values higher than 6.5 that prevail in the jejunum and the ileum of the gut (Wittaya-areekul et al., 2006; George and Abraham, 2006). Thus, chitosan-alginate complex erodes slowly in phosphate buffer at pH values higher than 6.5 and this behaviour leads to suppression of the initial drug release in the upper segments of GIT occurring for uncoated microparticles and controls release in the colon whereas pH value is in the range of 6.5–7.0 (Tapia et al., 2004). In addition, chitosan is degraded by the microflora that is available in the colon (Shin-ya et al., 2001; Sardar et al., 2003).

In the case of IBD, an enhanced uptake of administered particles by neutrophils, natural killer cells, mast cells, and regulatory T cells in the inflamed tissue were observed (Lamprecht et al., 2001a,b). This resulted in accumulation of the carrier system in inflamed area. From this point of view, it is advantageous to administer particles that tend to be attached to the mucus layer. Negatively charged particles may adhere more readily to the inflamed tissue because it has been reported that ulcerated tissues contain high concentrations of positively charged proteins that increase the affinity to the negatively charged substances. This was also confirmed by the study of Bernkop-Schnurch et al. (2001), in which anionic alginate showed more potent mucoadhesion in comparison with the cationic chitosan. Thus, an optimal particle size and polymers distribution for the design of a chitosan-alginate particulate carrier system must be chosen in order to prepare microparticles with high drug content and anti-inflammatory effect. Knowledge of the release profile and biodistribution of 5-ASA is essential to achieve optimal targeting when considering variables that determine release such as intraluminal pH and disease activity, which differ largely in patients with chronic IBD.

Considering above-mentioned, 5-ASA loaded chitosan-Ca-alginate microparticles were prepared using spray-drying method associated by ionotropic gelation/polyelectrolyte complexation. Physicochemical characterization, including microparticle size, morphology, polymers distribution, zeta potential, drug loading and drug–polymers interaction was performed as a function of the preparation procedure. The aim of this study was to investigate the influence of the polymers type on drug release and potential of the microparticles for colon delivery of 5-ASA. For this requirements, dissolution profile *in vitro* and biodistribution of 5-ASA contained in this new microparticulate system was studied after peroral administration to rats in which colonic inflammation was induced.

## 2. Materials and methods

### 2.1. Materials

Three types of sodium alginate (LF 10/60, fG 65–75%, viscosity 20–70 mPa s for 1% (w/v) solution; LF 120 M, fG 35–45%; viscosity 70–150 mPa s for 1% (w/v) solution, LF 10/60LS, fG 35–45%; viscosity 20–70 mPa s for 1% (w/v) solution) were purchased from Protanal FMC BioPolymers (Norway). Two types of chitosan with a same deacetylation degree ≥85% (low viscosity 342, viscosity of 1% (w/w) solution in acetic acid 20–100 mPa s, $M_w$ 150 kDa, $(R_G^2)^{1/2}$, 44 ± 5 nm and high viscosity 222, viscosity of 1% (w/w) solution in acetic acid 500–2000 mPa s, 659 kDa, $(R_G^2)^{1/2}$, 65 ± 8 nm) were obtained as a gift from France Chitine (France). 5-ASA was purchased from Fluka Chemie AG (Switzerland). Sodium salt of 2,4,6-trinitrobenzenesulphonic acid (TNBS) was purchased from Sigma–Aldrich, Inc. (Germany), *o*-dianisidine hydrochloride from Sigma–Aldrich, Inc. (USA) and hexadecyltrimethylammonium bromide (HTAB) from Sigma–Aldrich, Inc. (Germany).

Radiolabelling of 5-ASA was performed by Na[$^{131}$I] obtained from Biointernational (France). 1,2,4,6-Tetrachloro-3α,6α-diphenylglucouryl (IODO-GEN, Biointernational, France) was used as an oxidant. All other reagents were of analytical grade.

### 2.2. Preparation of microparticles

5-ASA loaded microparticles were prepared with slight modifications of the spray-drying method associated with polymer complexation/gelation (Coppi et al., 2001; Liu et al., 1997). A spray-drying technique was applied to 5-ASA/sodim alginate solutions to obtain spherical particles having a mean diameter less than 10 μm. Namely, aqueous dispersion (30 ml) of alginate (3%, w/w) and 5-ASA (0.5%, w/w), adjusted to pH 7.0 by 0.2 M NaOH, was infused into a spray dryer nozzle unit of Büchi Mini Spray Dryer B-191 (Büchi Laboratorius-Technik AG, Flawil, Switzerland) and continuously sprayed using an automatic infusion/withdrawal pump (model Sonceboz 3.1 A/pH, Switzerland) into 90 ml solution of chitosan (0.25%, w/w) and $CaCl_2$ (2.5%, w/v) in 1% (w/w) acetic acid, which was placed in the apparatus collector.

The conditions of the spray-drying process were: nozzle diameter 0.7 mm, aspirator pressure 100%, atomizer pressure 600 N l h$^{-1}$, flow rate 10 ml/min, inlet temperature 140 °C, outlet temperature 100 °C. The dispersion of microparticles was collected and they were allowed to harden under stirring (3000 rpm)

for at least 4 h at room temperature. The microparticles thus formed were separated by centrifugation at 3000 rpm for 15 min (Jouan B 3–11, France), washed with distilled water and freeze-dried at 0.250 mbar and −50 °C for 24 h (Bioblock Scientific Christ Alpha 1–4, Germany). Blank alginate-, Ca-alginate- and chitosan-Ca-alginate microparticles were prepared using the same conditions as for the drug-loaded particles. 5-ASA loaded alginate microparticles (termed as "temporary" microparticles) were also prepared by spray-drying of aqueous dispersion of alginate and 5-ASA using the same formulation and spray-drying conditions.

### 2.3. Physicochemical characterization of microparticles

For measurement of the freeze-dried microparticles' size, Beckman Coulter Multisizer (Coulter, USA) was used. The zeta potential of the particles was recorded using Malvern Zeta Sizer 2000 (Malvern Instruments Ltd., UK), while for calcium content to be determined, an atomic absorption spectroscopy (240 nm, ThermoSolaar S4, UK) was used (Fundueanu et al., 1998).

To evaluate the actual content of 5-ASA in the chitosan-Ca-alginate microparticles, at first, drug content in "temporary" microparticles was determined by dissolving an exactly weighed amount of microparticles in PBS pH 7.0 with magnetic stirring at room temperature under light and oxygen protection until complete dissolution. The yield of the spray-drying process was 55 ± 19%, calculated as an average value from five determinations from the six different series. These values were particularly satisfying knowing the generally low production yield encountered with laboratory scale spray-dryers (Giunchedi et al., 1996; De Jaeghere et al., 2001).

Real drug content was calculated as amount of 5-ASA in the microparticles in respect to the real amount of the chitosan-Ca-alginate microparticles obtained after freeze-drying (Coppi et al., 2001). These data were obtained in dissolution studies when a pH gradient-enzymatic method (described bellow) was used, where complete release of 5-ASA was observed.

5-ASA concentration was assayed by an UV/vis spectrophotometer at 300 nm in the clear supernatant solutions after centrifugation and separation of the microparticles (UV/vis spectrometer, Perkin-Elmer Lambda 16, USA).

Shape and surface characteristics of empty and 5-ASA loaded chitosan-Ca-alginate microparticles were studied by scanning electron microscopy (SEM; JEOL JSM-6301F Scanning Microscope, Tokyo, Japan). The localization of both the polymers in the microparticles, with regard to their respective distribution within the particle and/or wall material was determined using confocal laser scanning microscopy (Olympus light microscope Fluoview FU 300 Laser Scanning Confocal Imaging System, Paris, France) after fluorescent, FITC (for chitosan) and RBITC (for alginate), labeling of the polymers (Huang et al., 2002; Lamprecht et al., 2000a,b).

$^1$H NMR ($H_2O/D_2O$, 90/10, Bruker Advance DRX 500, Germany), FTIR (Bruker Vector 22, Germany), DSC (Mettler Toledo model 30TC 15, Mettler, Switzerland) and X-ray studies (Philips PW1830 model, Holland) were carried out in order to determine 5-ASA stability during microencapsulation and release in different pH mediums and drug–polymers interactions as well.

### 2.4. Drug release studies

Drug release studies were carried out in sealed glass vials at 37 °C and 75 horizontal strikes/min (horizontal shaker, Haake SWB20, Germany) where the suspension of 5-ASA loaded chitosan-Ca-alginate microparticles (6–8 mg/ml) was placed. To compare the drug release under different pH conditions, the experiments were performed in 0.1 M HCl (pH 1.2) to simulate fasted stomach and in phosphate buffer saline (pH 6.8) to simulate mid jejunum. To simulate passage through the stomach and the small intestine, release studies were carried out also by using a pH gradient/enzymatic method (EM) with some slight modifications (Tozaki et al., 1997, 2002; Zambito and Di Colo, 2003). This method was used also to deduce the influence of biodegradation mechanism on the drug release profile. Dissolution media and correspondent residence times included: stomach-120 min (pH 1.2, 0.1 M HCl), duodenum-10 min (pH 6, PBS), jejunum-120 min (pH 6.8, PBS) and suspension of fresh rat cecal content (33%, w/v) in bicarbonate buffer pH 7 until complete release of the drug (24 h). The pH of the buffer was adjusted to 7.0 by bubbling $CO_2$ gas through it prior to use. In this way, an anaerobic environment was maintained also. In the release medium, the following salts were included: $NaHCO_3$ (9.240 g/l), $Na_2HPO_4 \cdot 12H_2O$ (7.125 g/l), NaCl (0.470 g/l), KCl (0.450 g/l), $CaCl_2 \cdot 2H_2O$ (0.073 g/l), $MgCl_2 \cdot 6H_2O$ (0.087 g/l). The suspension was filtered through four layers of gauze.

The withdrawn samples in different time intervals were analyzed spectrophotometrically at 300–330 nm depending on the medium's pH value (UV Shimadzu 1601 Spectrometer, Japan).

Drug release constants were determined by different kinetic models (Higuchi, zero- and first order kinetics). To deduce the mechanism of drug release from the microparticles, the release data were fitted to the general exponential equation which is used to describe the drug release behaviour from swellable polymers: $M_t/M_0 = kt^n$ (Ugwoke et al., 1997); where $M_t/M_0$ is the fraction of the drug released [$\leq 0.6$) at time $t$; $n$ is an exponent related to the release mechanism and $k$ denotes the constant incorporating structural and geometric characteristics of the drug–polymer/system. This equation was used frequently in predicting the relative importance of Fickian ($n = 0.43$) and Case II ($0.43 < n < 0.85$) transport in anomalous diffusion, and Super Case II transport where $n \geq 1.0$ (Ritger and Peppas, 1987).

### 2.5. Biodistribution studies

#### 2.5.1. Induction of colonic inflammation/animals treatment

Biodistribution studies were carried out on Wistar male rats aged 12–15 weeks and weighing 230–250 g. Animals were housed in an air-conditioned room at 22 ± 3 °C, 55 ± 5% humidity, 12 h light/dark cycles and allowed free access to water and laboratory chow for the duration of the studies. To induce the model of chronic inflammation in the rat colon, the method described by Morris et al. (1989) was followed. Briefly, rats were arbitrarily separated into treatment groups, fasted for 24 h

with free access to water and then lightly anaesthetized with ether. A graduated rubber canula was inserted rectally into the colon such that the tip was 8 cm proximal to the anus. TNBS (150 mg/kg body weight) dissolved in 50% ethanol (v/v) was instilled into the lumen of the colon through the rubber probe (total volume 0.5 ml solution). A control group received 0.5 ml 0.9% (w/v) saline administered as before.

The induction and development of inflammation were monitored periodically during 3 weeks. Rats (in groups of 5) were sacrificed with ether every day during the 1st week and the 8th, 14th and 21st day of administration. The stomach, upper intestine, cecum, colon, rectum, liver and the kidneys were removed. The development of inflammation was evaluated in respect to the clinical activity score, macroscopic and pathohistological changes, colon weight/body weight ratio, myeloperoxidase activity and distribution of CD3 T and CD79 B lymphocytes.

*2.5.2. Determination of colon/body weight ratio*

The rats were killed, then the abdomen was opened and the distal colon was rapidly excised and opened longitudinally along the mesenteric edge. The colon was washed with 0.9% (w/v) saline and placed with the mucosal surface upward over a glass plate chilled with ice. The ratio of the 8 cm segment distal colon weight was calculated as an index of colonic tissue oedema (Yue et al., 1996).

*2.5.3. Assessment of macroscopic ulceration and histological evaluation*

Gross mucosal damage was scored on a 0–3-grade scale by a single observer blind to the treatment (Rodriguez et al., 2001). Damage was scored as follows: score 0 represented no damage; score 1-localized hyperaemia with slight or minimal ulceration; score 2-linear ulcers and one or two regions with ulcers of 1–2 cm; score 3-severe ulceration (regions with ulcers >2 cm). After scoring, two tissue samples were excised from each colon and maintained in formaldehyde (10%, v/v) for microscopic studies. When visible ulceration or inflammation was present, at least one of the samples from the affected region was taken. These tissue samples were processed routinely and embedded in paraffin. Sections (5 μm) were stained with haemotoxylin and eosin. Microscopic assessment by light microscope was performed blind on coded slices. Histological damage was also scored on a 0–3 scale as follows: score 0-no damage; score 1-no significant inflammation, score 2-moderate inflammatory infiltrate (one or two regions affected with the number of neutrophils slightly increased), score 3-severe inflammatory infiltrate (several inflamed regions with many neutrophils).

*2.5.4. Clinical activity score system*

Colitis activity was quantified with a clinical score assessing weight loss, stool consistency and rectal bleeding as applied by Hartmann et al. (2000) and Lamprecht et al. (2001a,b). No weight loss was counted as 0 point, 1–5% as 1 point, 5–10% as 2 points, 10–20% as 3 points and >20% as 4 points. For stool consistency, 0 point was given for well-formed pellets, 2 points for pasty and semiformed stools that did not stick to the anus and 4 points were given for liquid stools that stick to the anus. Bleeding was scored as 0 point for no blood, 2 points for positive finding and 4 points for gross bleeding. The mean of these scores was forming the clinical score ranging from 0 (healthy) to 4 (maximal activity of colitis).

*2.5.5. Myeloperoxidase activity*

The measurement of the myeloperoxidase activity was performed to quantify the severity of the colitis. It is a reliable index of inflammation caused by infiltration of activated neutrophils into the inflamed tissue. Activity was analyzed according to Krawiscz et al. (1984). Briefly, distal colon specimen was minced in 1 ml of HTAB buffer (0.5% in 50 mM phosphate buffer) on ice and homogenized. The homogenate was sonicated for 10 s (MicrosonTM XL 2007, Ultrasonic Cell Disruptor, Microsonix Inc., USA), freeze-thawed three times and centrifuged at 12,000 rpm for 3 min (Eppendorf AG 22331, Germany). Myeloperoxidase activity in the supernatant was measured spectrophotometrically. Supernatant (0.1 ml) was added to 0.167 mg/ml of *o*-dianisidine hydrochloride and 0.0005% hydrogen peroxide, and the change in absorbance at 460 nm was measured. One unit of myeloperoxidase activity was defined as the amount that degraded 1 μmol of peroxidase per minute at 25 °C. The results were expressed as U/mg tissue (Jagtap et al., 2004).

*2.5.6. Distribution of CD3 T and CD79 B lymphocytes*

Tissue samples of colon were formalin fixed and embedded in paraffin wax. The immunohistochemical (ABC) method was performed by using monoclonal antibody CD3 T lymphocytes (DAKO) in 1:50 dilution and monoclonal antibody CD79αcy B lymphocytes (DAKO) in 1:50 dilution.

*2.5.7. Experimental design*

Biodistribution of radiolabelled [$^{131}$I]-5-ASA after peroral administration in a form of chitosan-Ca-alginate microparticles (group I) was followed in comparison with biodistribution of [$^{131}$I]-5-ASA administered per orally as an aqueous suspension (group II). 5-ASA formulations were administered in the period of the most intensive inflammation, i.e. the sixth day of TNBS administration. Thus, to two groups of rats fasted for 24 h, 1 ml saline containing 0.023 mg/g [$^{131}$I]-5-ASA and amount of particles equivalent to 0.023 mg/g [$^{131}$I]-5-ASA were administered orally via polyethylene cannula under light ether anaesthesia. Biodistribution of [$^{131}$I]-5-ASA was followed periodically within 48 h (1st, 3rd, 5th, 10th, 24th and 48th hour). The animals were sacrificed, the blood was collected and different organs and tissues were removed. The GIT was separated into the stomach, upper intestine (including proximal jejunum, distal jejunum, proximal ileum and distal ileum) and colon (including ascending, transverse and descending colon). The contents of those parts were collected and the remaining gastrointestinal tract sections were thoroughly rinsed. The radioactivity in the stomach, small intestine with Payer's patches (PP) and mesentery, colon with PP, appendix and mesentery, liver, spleen, kidney, lungs, heart and blood (2 ml per animal) were determined using a scintillation counter (NaI (TL); "well" counter Scaler Type N 529 D, EKCO Electronics, UK). The number of

Table 1
Content and examined parameters of 5-ASA loaded chitosan-Ca-alginate microparticles

| Series | Alginate | | Chitosan | | 5-ASA content (theoretical content = 14.28%) % | Particle size (μm) | Zeta potential (mV) | $Ca^a$-content % |
|---|---|---|---|---|---|---|---|---|
| | Type | % | Type | % | | | | |
| S-I | A1[b] | 3 | LV[c] | 0.25 | 8.86 ± 0.69 | 6.2 ± 2.21 | −30.7 ± 1.8 | 3.6 ± 0.2 |
| S-II | A2[b] | 3 | LV[c] | 0.25 | 9.93 ± 0.23 | 6.5 + 1.09 | −28.0 + 2.1 | 3.9 + 0.5 |
| S-III | A3[b] | 3 | LV[c] | 0.25 | 9.79 ± 0.81 | 8.6 + 3.21 | −27.0 ± 1.2 | 3.5 ± 0.2 |
| S-1 | A1[b] | 3 | HV[c] | 0.25 | 10.91 ± 0.42 | 6.3 ± 2.24 | −28.5 ± 1.1 | 3.7 ± 0.2 |
| S-2 | A2[b] | 3 | HV[c] | 0.25 | 7.89 ± 0.81 | 7.4 ± 3.32 | −21.5 ± 1.0 | 3.9 ± 0.3 |
| S-3 | A3[b] | 3 | HV[c] | 0.25 | 10.14 ± 0.74 | 8.4 ± 3.35 | −23.7 ± 1.5 | 3.5 ± 0.1 |

[a] $CaCl_2$ concentration in the cross-linking medium 0.25% (w/w).
[b] A1: fG 65–75%, 20–70 mPa s; A2: fG 35–45%, 70–150 mPa s; A3: fG 35–45%, 20–70 mPa s (viscosity of aqueous solution 1%, w/v).
[c] LV, low viscosity: 20–100 mPa s (1%, w/w in solution of acetic acid 1%, w/v), $M_m$ 150 kDa, $(R_2G)^{1/2}$ 44 ± 5 nm, $d_d > 85\%$; HV: high viscosity: 500–200 mPa s (1%, w/w in solution of acetic acid 1%, w/v), Mm 659 kDa, $(R_2G)^{1/2}$ 65 ± 8 nm, $d_d > 85\%$.

animals ($n$) per group at a given time point of biodistribution studies was 5. In order to eliminate the radioactivity in the tissues, organs and central circulation due to $^{131}I$ only because of possible iodolysis, preliminary biodistribution studies of $^{131}I$-solution were performed after oral administration to group of rats. Accumulation of $^{131}I$ in the thyroid (approximately 99%) at each time point of study was confirmed, so the eventual radioactivity in the tissues, organs and central circulation due to $^{131}I$ only was eliminated (Mladenovska et al., 2002, 2003).

*2.5.8. Radiolabelling of 5-ASA with radioactive iodine, $^{131}I$*

Radiolabelling of 5-ASA was performed by a radioactive iodine in a form of Na[$^{131}$I]. The conversion of Na[$^{131}$I] was performed by an oxidant, IODO-GEN (1,2,4,6-tetrachloro-3α,6α-diphenylglucouryl). Reaction went on in PBS pH 7.0 with 565 μCi $^{131}I$ per 506 mg 5-ASA during 10 min. Radiochemical purity was determined by instant thin-layer chromatography and 0.1 mol/l HCl as a mobile phase (ITLC-SG, scan detector VCS-101 VEENSTRA instruments, UK). The product stability was followed within 8 days.

## 3. Results and discussion

### *3.1. Physicochemical characterization of microparticles*

Negatively charged particles from −21.5 ± 1.0 to −30.7 ± 1.8 mV were prepared, with size from 6.2 ± 2.2 to 8.6 + 3.2 μm and calcium content from 3.6 ± 0.2% to 3.9 ± 0.5%. It must be emphasized that the zeta potential of the particles was determined in a diluted phosphate buffer (0.0001 M) with pH 6.8 in order to simulate *in vivo* conditions. Most of the studies carried out in patients with IBD confirmed that colon pH was not changed (Ewe et al., 1999; He et al., 1999).

Real drug content ranged from 7.89 ± 0.81% to 10.91 ± 0.42%, respectively (Table 1), which is satisfactory 5-ASA content comparing with the theoretical value (14.28%).

Acceptable spherical morphology was observed, but also flattened, disk-shaped particles. The surface appears smooth with low porosity (Fig. 1). By imaging with CLSM, the chitosan was localized dominantly in the particle wall, with a low quantity homogeneously distributed throughout the particle matrix. Homogeneous distribution of the alginate throughout the particle was observed with a heterogeneous deposition at the alginate/chitosan interface (Fig. 2).

Previously performed, $^1$H NMR studies confirmed that the formulation and the technology applied ensure 5-ASA stability during microencapsulation and in simulated *in vivo* drug release conditions when different pH mediums were used. No degradation of 5-ASA occurred when working in adequate conditions, such as light protection, freshly prepared solutions, use of nitrogen to prevent the oxidative-self coupling of 5-ASA moieties and $CO_2$ in drug release mediums to simulate anaerobic conditions. In the FTIR spectra of 5-ASA loaded Ca-alginate microparticles, the characteristic peaks of 5-ASA were not altered indicating no

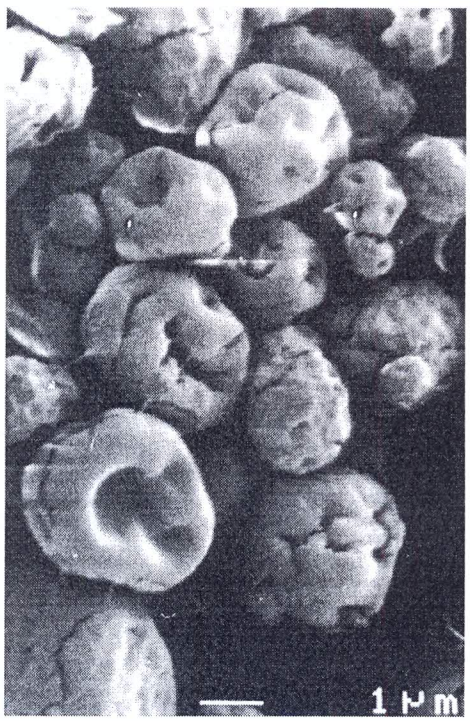


Fig. 1. SEM of 5-ASA loaded chitosan-Ca-alginate microparticles.

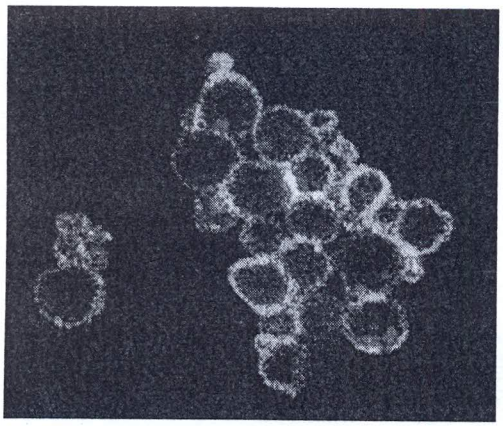

Fig. 2. CLSM of 5-ASA loaded chitosan-Ca-alginate microparticles; image obtained by superposition of FITC labelled chitosan and RBITC labelled alginate.

covalent interaction between the drug and the polymer. X-ray and DSC studies indicated molecularly dispersed drug within the particles (data not shown).

### 3.2. Dissolution studies

As was previously mentioned, the formulation and the technological approach in the preparation of 5-ASA loaded microparticles have to provide a control in the 5-ASA release for a relatively long period and/or to delay the drug release in the stomach. These expectations were based on the physicochemical properties of the polymers, the mucoadhesivity and pH sensitive solubility at first and on the physicochemical properties of 5-ASA also, i.e. its predominantly anionic ($pK_{a_1}$ 2.3, $pK_{a_2}$ 5.4) properties and low octanol-water and chloroform-water partition coefficients ($\log K_p$: 1.4 and 1.5, respectively) (Zerrouk et al., 1998; Zhou et al., 1999a,b).

Results related to the 5-ASA release from the formulations in which different combinations of polymers were used and in mediums with different pH values, with and without enzymes,

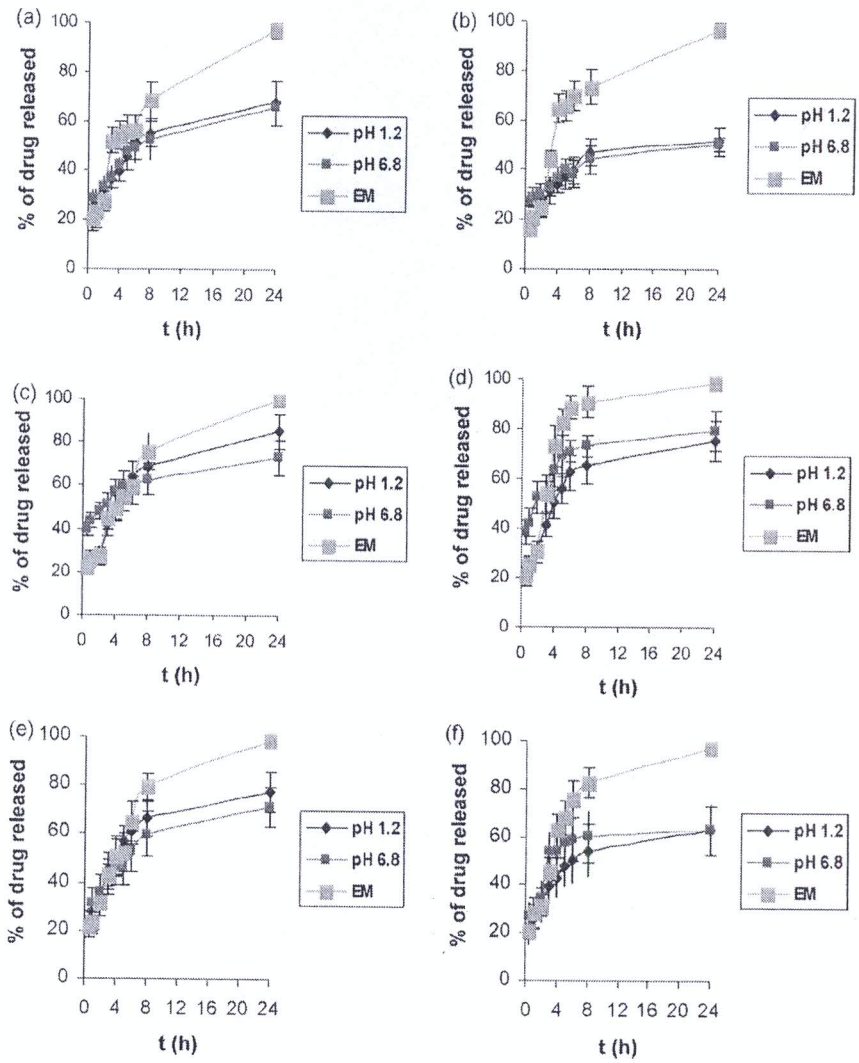


Fig. 3. 5-ASA release from chitosan-Ca-alginate microparticles in different dissolution mediums; S-I (a), S-1 (b), S-II (c), S-2 (d), S-III (e), S-3 (f).

were in accordance with these expectations (Fig. 3). The drug release was prolonged for a period of 24 h in anaerobic conditions, which included presence of enzymes, salts and ionic strength specific to the colon. In most of the formulations (S-I, S-1, S-III, S-3) in all mediums tested an initial 5-ASA release between 16% and 27% was observed in the first 30 min, which can be probably explained by the release of 5-ASA localized near or on the particles' surface.

In conditions simulating gastric content the 5-ASA release during 2 h was between 27% and 35%. Exception were the series of microparticles prepared with higher viscosity alginate rich in mannuronic acid (S-II, S-2), where 5-ASA release in the initial phase and in the phase of continuous release was relatively faster with approximately 40% and 50% in the initial phase and during 2 h, respectively.

At increasing pH, the increased deprotonation of chitosan did not result in faster drug release. In fact, the 5-ASA release in pH 6.8 was similar or non-significantly lower than the one in pH 1.2. Mathematical analysis (presented in addition) pointed to the release governed by the dissolution of 5-ASA and diffusion through the hydrated paths in the matrix formed by polymers swelling. In addition, the limited solubility of 5-ASA in the matrix region where diffusion occurs and a higher solubility at 37 °C in 0.1 mol/l HCl (8.65 mg/ml) in respect to the one in phosphate buffer with pH 6.8 (3.94 mg/ml) (Turkoglu and Ugurlu, 2002) contribute also to the relatively slower 5-ASA release in pH 6.8. For, e.g., during 2 h in formulation S-I, 27.43 ± 3.42% of the drug were released in the acidic medium, while for the same period, 33.82 ± 2.99% were released in the alkaline medium. Six hours latter, i.e. the eighth hour, the percent of drug released was 54.84 ± 3.65% and 49.09 ± 3.75%, respectively.

Colonic salts and enzymatic activity modified the release-determining factors probably by increasing the internal matrix pH, porosity and degradation rate. During 24 h complete drug release was observed in all series of 5-ASA loaded chitosan-Ca-alginate microparticles (Fig. 3).

At pH 1.2, alginate is protonated into the insoluble form of alginic acid displaying swelling properties that prolong the drug release (Gombotz and Wee, 1998). When freeze-dried chitosan-Ca-alginate microparticles exposed to acidic pH, the protonated amino groups of 5-ASA are expected to be electrostatically bonded to the dissociated carboxyl groups of alginate. The release can be hindered by chitosan also; its positively charged amino groups can strongly interact with alginate and 5-ASA. These highly cooperative ionic bonds between the oppositely charged polymers, which are main driven force in binding and localization of chitosan into the particles, and the existence of inter- and intramolecular hydrogen bonds and hydrophobic forces between the drug and the polymers can increase the mechanical strength of the gel network and decrease its porosity/permeability. Therefore, the swelling kinetics will be much slower, so the erosion of alginate matrix and 5-ASA release as well. In addition, the cooperative bonds between the oppositely charged polymers are expected to result in non-significant loss of chitosan in acidic medium despite its cationic properties, which can additionally contribute to the slower 5-ASA release in alkaline pH. Namely, the presence of chitosan in the system is of crucial importance for slower swelling kinetics caused by osmotic changes and/or $Ca^{2+}$ exchange in the presence of lactate, citrate, phosphate and high concentrations of magnesium and sodium ions (Gaserod et al., 1998, 1999; Zambito and Di Colo, 2003). When entering into the colon, where pH is between 6.4 and 7.0, the increased deprotonization of chitosan's amino group and the degradation mediated by bacterial enzymes specific to the colon can decrease the intensity of the interactions into the particles. However, the electrostatic forces occurring between the deprotonated carboxyl groups of alginate and positively charged amino groups of 5-ASA, and the additional hydrogen bonds and van der Waals' forces could extend the 5-ASA release. Low 5-ASA solubility in this medium could additionally contribute to the slower release from the particles. In fact, 5-ASA release could be controlled by the swelling kinetics and/or $Ca^{2+}$ exchange. Depending on the cross-linking degree and/or swelling kinetics of alginate gel-matrix and biodegradation rate of chitosan, alginate matrix will hydrolyze with a rate that controls the 5-ASA release.

As one can see, 5-ASA release from the series of chitosan-Ca-alginate microparticles prepared with alginate rich in mannuronic acid (M) was faster in all release mediums than the one in the series prepared with alginate rich in guluronic acid (G) (Table 2). For, e.g., the percent of 5-ASA released in alkaline medium during 8 h in series prepared with G-rich alginate (S-I) was 49.09 ± 3.75%, while for the same period, 59.84 ± 5.44% were released from the series of microparticles prepared with M-rich alginate (S-III) with the same viscosity as G-rich alginate. Notice that the same type of chitosan was used for preparing both the formulations. These results could be explained by the higher cooperation between the guluronic acid units provided by calcium chloride. Namely, it has been reported that alginate gels with a high G content exhibit high porosity, low shrinkage during gel formation and do not swell after drying. With increasing M content, the gels become softer and more elastic; they shrink more and their porosity is reduced. They swell after drying and dissolve easily in the presence of phosphate ions (Acarturk and Takka, 1999; Takka and Acarturk, 1999; Khairou and Hassan, 2002). The gelation takes place by forming egg-box junctions to associate the calcium ions with the GG blocks of the alginate chain. The guluronic acid conformation gives suitable distance between the carboxyl and hydroxyl groups to give a high degree of coordination of the calcium. The alginates rich in guluronic acid form more rigid gels, which would be

Table 2
Kinetic constants ($k$) ± S.D. and determination coefficients ($r^2$) obtained by linear regression of cumulative amount released *vs.* square root of time ($n = 6$)

| Series | $K$ (%h$^{-1/2}$) ($r^2$) | | |
|---|---|---|---|
| | pH 1.2 | pH 6.8 | EM |
| S-I | 8.61 ± 1.23 (0. 954) | 6.35 ± 1.54 (1.00) | 13.50 ± 3.65 (0. 959) |
| S-II | 10.10 ± 2.36 (0. 979) | 8.51 ± 2.38 (1.00) | 13.82 ± 3.99 (0. 968) |
| S-III | 9.72 ± 1.65 (0. 989) | 8.31 ± 2.87 (1.00) | 13.85 ± 3.57 (0. 981) |
| S-1 | 6.85 ± 1.07 (0. 997) | 5.32 ± 1.33 (1.00) | 13.00 ± 2.99 (0. 962) |
| S-2 | 9.56 ± 1.68 (0. 989) | 7.26 ± 1.65 (1.00) | 12.73 ± 2.98 (0. 969) |
| S-3 | 7.98 ± 1.98 (0.954) | 6.98 ± 1.36 (1.00) | 13.05 ± 3.01 (0.982) |

less prone to erosion and the drug release would be slower. In addition, $Ca^{2+}$ release/exchange from the G-rich alginate gels is characterized by a biphasic release profile; an initial phase of relatively fast release of $Ca^{2+}$ bonded to the carboxyl groups of the mannuronic acid, followed by a phase of relatively slower release of $Ca^{2+}$ bonded to the guluronic units (Liu et al., 2002). Also, the amount of bound chitosan in such matrices is greater than the one in matrices prepared of M-rich alginate (Gaserod et al., 1998, 1999), which can also contribute to the slower drug release.

Viscosity of the alginate did not affect the drug release significantly. Namely, during 8 h in pH 6.8, 59.84 ± 5.44% of 5-ASA were released when lower viscosity alginate was used (S-III), while for the same period, 62.81 ± 3.01% of the drug were released when the higher viscosity alginate was used (S-II) with the same mannuronic to guluronic units ratio.

From the results obtained, it was seen that the viscosity/molecular weight of chitosan did not affect the drug release significantly. For, e.g., during 24 h, 73.18 ± 8.01% of 5-ASA were released in formulation prepared of low viscosity chitosan (S-II), while in the series prepared of high viscosity chitosan (S-2) in the same period, 79.33 ± 7.69% of the drug were released in pH 6.8. Notice that the same type of alginate was used.

In order kinetic constants of drug release to be determined, the percent of the drug released was plotted *versus* time by using mathematical models of first order- and zero order kinetic and Higuchi's model of diffusion. Upon checking the results according to the values of the determination coefficients ($r^2$), the best fits for all the formulations were obtained by Higuchi's model of diffusion, where the rate constants are obtained from the slope of linear regression of cumulative amount released *versus* square root of time (% $h^{-1/2}$). This was also confirmed by the differential mathematical test according to which, the linear regressions of drug release rate ($dM/dt$) *versus* reciprocal value of the drug released ($1/M_t$) in all series and drug release mediums had higher values ($0.817 \leq r^2 \leq 0.962$) in comparison with the linear regressions of $dM/dt$ *versus* $M_t$ ($0.509 \leq r^2 \leq 0.790$). Linear square-root time kinetics of all plots suggested release governed by the drug dissolution and diffusion in the aqueous path created in matrix by polymer hydration (Table 2).

Table 3
Kinetic constants ($k$), diffusional exponents ($n$) and determination coefficients ($r^2$) by linear regression of $\ln(M_t/M_\infty)$ *vs.* $\ln t \pm$ S.D. ($n = 6$)

| Series | $n \pm$ S.D. | $k \pm$ S.D. | $r^2$ |
|---|---|---|---|
| S-I | 0.456 ± 0.017 | 0.398 ± 0.027 | 0.951 |
| S-II | 0.439 ± 0.002 | 0.465 ± 0.054 | 0.956 |
| S-III | 0.500 + 0.004 | 0.456 ± 0.043 | 0.978 |
| S-1 | 0.617 ± 0.016 | 0.226 ± 0.040 | 0.950 |
| S-2 | 0.472 ± 0.013 | 0.386 ± 0.019 | 0.929 |
| S-3 | 0.476 ± 0.011 | 0.385 ± 0.010 | 0.966 |

The kinetics of release data was assessed also by linear regression of $\ln(M_t/M_0)$ on $\ln t$ in a pH gradient-enzymatic method, where 60% of the drug was released before the exchange of the phosphate buffer with buffered cecal content. Values for the diffusional exponent were between 0.439 and 0.617 for all formulations indicating non-Fickian release behavior in the initial release phase controlled by a combination of diffusion and chain relaxation mechanisms (Table 3). In the phase of slow and constant release (in which the complete 5-ASA content was released) in the medium containing cecal content, other drug release mechanisms, such as erosion and biodegradation, cannot be excluded.

### 3.3. Assessment of the induced colonic inflammation

TNBS model appeared to show high correlation between pathohistological, immunological and clinical features of the inflammation in IBD (Tozaki et al., 1999, 2002; Rodriguez et al., 2001). Simplicity, reproducibility and time- and dose related development of inflammation were main advantages for using this model in following biodistribution of 5-ASA loaded in chitosan-Ca-alginate microparticles.

Namely, macroscopic and histological changes of the colon the first day of administration included appearance of local hyperemia, ulcers smaller than 1 cm and mild inflammatory infiltrate. In the period of the most intensive inflammation, i.e. the sixth day of administration, marked thickening of the intestinal wall associated with hemorrhages, severe cellular infiltration

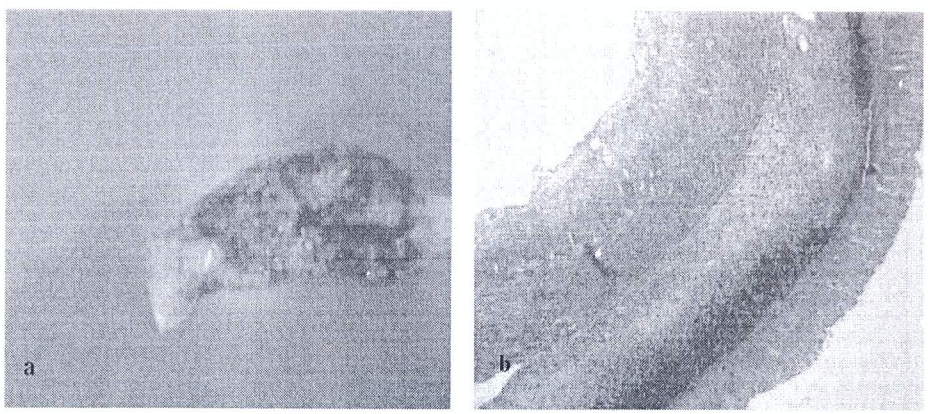


Fig. 4. Macroscopic and microscopic images of rat colon the sixth day of TNBS in ethanol administration. Optical micrograph shows the mucosa with serious inflammatory infiltrate (a) and necrotic changes (b).

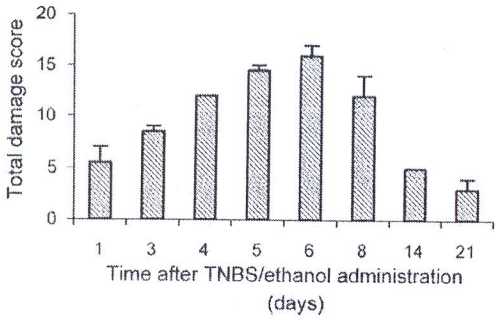


Fig. 5. Effect of TNBS/ethanol on the total damage score from the first to the 21st day of administration; each bar is an average value ± S.D. of five animals; total damage score 16 ± 1.0 *vs.* 0 in the control group.

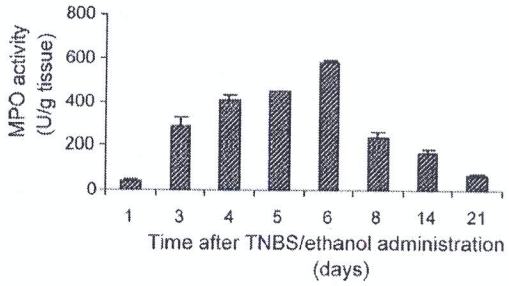


Fig. 7. Effect of TNBS/ethanol on the MPO activity from the first to the 21st day of administration; each bar is an average value ± S.D. of five animals. All the data are significantly higher ($p < 0.01$) than the average value of the control group (34.03 ± 4.09 U/g).

(including polymorphonuclear leucocytes, eosinophils, lymphocytes and granulocytes), epithelial exfoliation and ulcer that exceed 2 cm were seen (Fig. 4).

The inflammation was spread over the mucosa, submucosa, muscle layer and included serosa. All rats suffered from diarrhea after administration of TNBS. However, this was not the case for those rats treated with saline. A narrowing of the lumen of the colon adjacent to the inflamed sites with a proximal dilation of the bowel was also seen in the TNBS-treated rats, but generally the colon was not perforated.

In the same period, i.e. the sixth day of TNBS administration, the total damage score was the highest, 15 ± 2 *versus* 5 ± 1 in the first day of administration and 0 for the control group (Fig. 5). From the 8th to the 21st day of administration the damage score decreased and the 21st day of administration it was 3 ± 1. During the study, the colon weight/total body weight ratio increased from 13 ± 1 mg/mg the first day of administration to 30 ± 6 mg/mg the sixth day of administration, while on the 21st day the ratio decreased to 11 ± 1 mg/mg (Fig. 6). Activity of MPO correlated with these observations entirely and the lowest activity on the first day of administration (41.23 ± 11.65 U/g) and the maximal activity on the sixth day of administration (578.48 ± 10.58 U/g) was observed, while on the 21st day it was 63.92 ± 11.9 U/g (Fig. 7). In the control group, the colon weight/total body weight ratio was 8.5 ± 0.5 mg/mg during the study, while the activity of MPO was 34.09 ± 4.09 U/g. CD3 T lymphocytes and CD 79 B lymphocytes within the control group were mainly visible along the epithelia from *lamina epithelialis* and diffuse in *lamina propria* of the colon. With the development of inflammation their number significantly decreased and in the areas covered with ulcers as a result of necrotic and apoptotic changes they could not be observed.

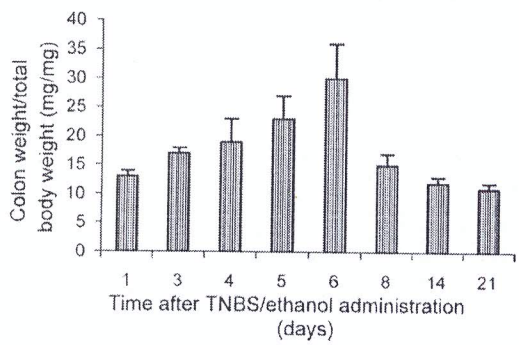


Fig. 6. Effect of TNBS/ethanol on the colon weight/total body weight ratio from the first to the 21st day of administration; each bar is an average value ± S.D. of five animals. All the data are significantly higher ($p < 0.01$) than the average value of the control group (0.0085 ± 0.0005 mg/mg).

### 3.4. Biodistribution studies

Knowledge for the unique transport, metabolic and elimination processes of 5-ASA correlates the absorption and pharmacology of 5-ASA and places the intestinal metabolism as a key process in the activity mechanism (Zhou et al., 1999a,b). This mechanistic principle explains the results related with the biodistribution of 5-ASA formulations tested in this study.

5-ASA formulations, aqueous suspension and 5-ASA loaded microparticles were perorally administered in the period of the most intensive inflammation, i.e. the sixth day of TNBS administration. One hour after peroral administration of 5-ASA loaded chitosan-Ca-alginate microparticles (group I, $n = 5$), 82.57 ± 0.03% of the total radioactivity present in all organs, tissues and blood was detected in the stomach. The percent of radioactivity appearing in the same region in the group of rats treated with 5-ASA suspension (group II, $n = 5$) 1 h after was 40.06 ± 0.02% (Fig. 8). The total radioactivity present in other organs separately and in the blood was low and non-significant in the group treated with microparticulate 5-ASA (e.g. 8.13 ± 0.17% in the upper intestine and 2.95 ± 0.33% in the colon), while in the group treated with suspension of 5-ASA, it was higher (18.67 ± 0.01% and 9.37 ± 0.21%, respectively). The percent of radioactivity present in the blood and the liver in the group treated with 5-ASA suspension was significantly higher than the one in the group treated with microparticulate 5-ASA (5.81 ± 0.46% in the blood and 14.69 ± 0.74% in the liver in the group II *versus* 0.11 ± 0.10% and 0.63 ± 0.11% in the group I), which can be explained by greater amount of systemically absorbed 5-ASA when as suspension administered. In addition, the percent of radioactivity present in the kidneys, which was 4.84 ± 0.01% in the group II *versus* 0.78 ± 0.04% in the group I confirmed the above-mentioned observation. The radioactivity present in the spleen in the group I (3.77 ± 0.07%) can be explained by the translocation of the smaller particles

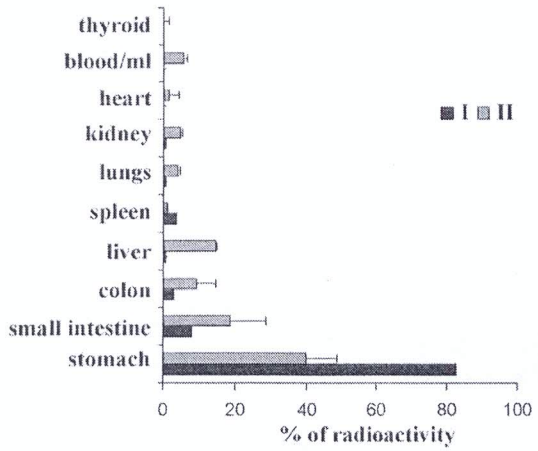


Fig. 8. Biodistribution of [$^{131}$I]-5-ASA loaded chitosan-Ca-alginate microparticles, 1 h after peroral administration to Wistar rats with TNBS induced ulcerative colitis; 5-ASA loaded microparticles (group I) and 5-ASA suspension (group II).

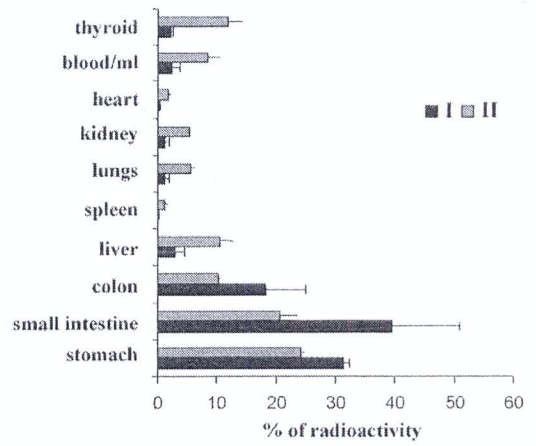


Fig. 10. Biodistribution of [$^{131}$I-5-ASA loaded chitosan-Ca-alginate microparticles, 5 h after peroral administration to Wistar rats with TNBS induced ulcerative colitis; 5-ASA loaded microparticles (group I) and 5-ASA suspension (group II).

also, after being taken up into PP and transported *via* the mesentery lymph supply and lymph nodes to the systemic lymphoid tissues, such as spleen.

The radioactivity in the stomach 3 h after administration of $^{131}$I-5-ASA loaded chitosan-Ca-alginate microparticles was 42.62 ± 4.86% and in the upper intestine and colon 27.84 ± 4.73% and 10.76 ± 1.49%, respectively. The percent of radioactivity in the group II in the same regions was 36.38 ± 2.16%, 31.74 ± 3.86% and 3.54 ± 0.81%, respectively (Fig. 9). The percents of radioactivity in other organs and tissues, such as liver (6.98 ± 0.57% in the group I *versus* 8.79 ± 0.48% in the group II), blood (2.71 ± 0.17% in the group I *versus* 7.59 ± 0.25% in the group II) and kidneys (2.32 ± 0.31% in the group I *versus* 4.75 ± 0.25% in the group II) pointed to the higher amount of 5-ASA absorbed (as a parent compound or metabolite) and eliminated when 5-ASA as a suspension was administered.

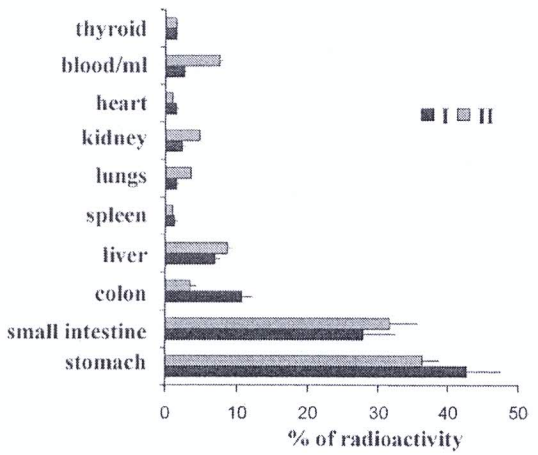


Fig. 9. Biodistribution of [$^{131}$I]-5-ASA loaded chitosan-Ca-alginate microparticles, 3 h after peroral administration to Wistar rats with TNBS induced ulcerative colitis; 5-ASA loaded microparticles (group I) and 5-ASA suspension (group II).

Five hours after administration of $^{131}$I-5-ASA loaded particles, radioactivity in the upper intestine and colon was 39.55 ± 11.23% and 18.29 ± 6.65%, while in the group treated with 5-ASA suspension, it was 20.71 ± 3.0% and 10.30 ± 0.17%, respectively (Fig. 10). In this period of time, again, significantly higher percents of radioactivity in the other organs and tissues, such as liver, lungs, kidneys and blood in the group II were observed.

Furthermore, the high radioactivity in the thyroid, present in the group II and absent in the group I, pointed also to the higher amount of systemically absorbed (as a parent drug or metabolite) 5-ASA when as suspension administered. Results related to the stability of [$^{131}$I]-5-ASA complex in the phase of radioactive labelling pointed to a very low percent of free $^{131}$I (<5%) (Fig. 11). This data and the fact that a relatively high radioactivity in the thyroid occurred 5 h of administration dominantly in the group treated with 5-ASA suspension, 11.86 ± 2.40% *versus* 2.28 ± 0.38% in the group I, support the above-mentioned observation.

Intention for colon-specific delivery and controlled release of 5-ASA (associated by adhesion of the particles in this region) was confirmed by the results after 10 h of administration. In this period, the radioactivity in the colon in the group I was very high, 45.64 ± 11.06% *versus* 16.09 ± 5.48% in the group in which

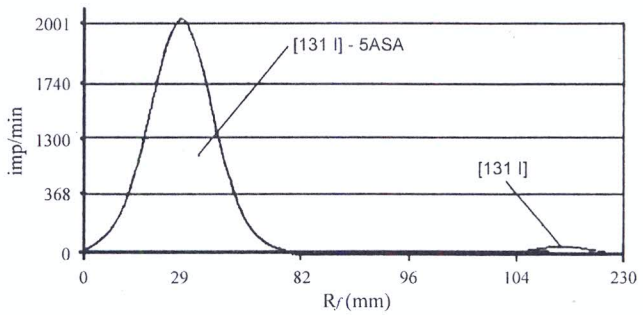


Fig. 11. ITLC of [$^{131}$I]-5-ASA in 0.1 mol/l HCl.

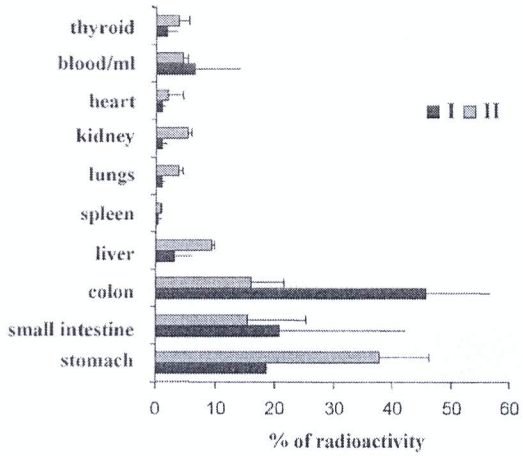


Fig. 12. Biodistribution of [$^{131}$I]-5-ASA loaded chitosan-Ca-alginate microparticles, 10 h after peroral administration to Wistar rats with TNBS induced ulcerative colitis; 5-ASA loaded microparticles (group I) and 5-ASA suspension (group II).

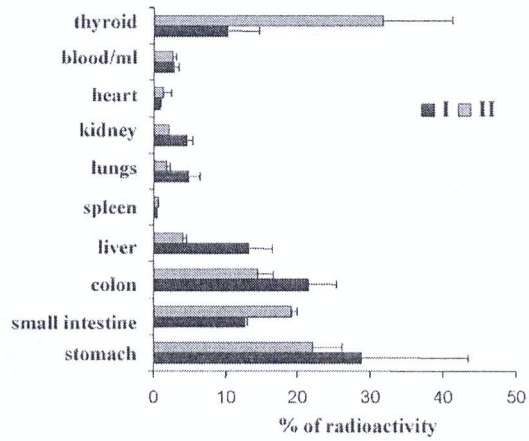


Fig. 14. Biodistribution of [$^{131}$I]-5-ASA loaded chitosan-Ca-alginate microparticles, 48 h after peroral administration to Wistar rats with TNBS induced ulcerative colitis; 5-ASA loaded microparticles (group I) and 5-ASA suspension (group II).

5-ASA suspension was administered (Fig. 12). The radioactivity can be probably attributed to the radioactivity of 5-ASA loaded and released in/from microparticles and metabolized in the intestine as well.

The radioactivity in the upper regions of GIT (seen in group II the 10th hour of administration) and in both groups after 24 h (Fig. 13) can be explained by the presence of intestinally and systemically metabolized 5-ASA. According to the literature data (Sandborn and Hanauer, 2003), the absorbed portion of 5-ASA is almost completely acetylated in the gut wall and in the liver, and the rate of acetylation, and hence the concentration of parent drug and metabolite in the wall and systemic circulation, is dependent on the acetylator status. The elimination half-life of 5-ASA in humans is reported to be 1 h (40–50% bound to plasma proteins); the acetylated metabolite has a half-life of up to 10 h and is about 80% bound to plasma. So, the radioactivity in the stomach after 48 h may be partly explained by a presence of 5-ASA metabolite. However, the gastric retention of 5-ASA loaded microparticles achieved by mucoadhesion and sticking of polymers to water-soluble proteins in the stomach may also be a reason for high radioactivity in the stomach after 24 and 48 h of administration in the group I (Figs. 13 and 14). This may prolong the resident time in the stomach until mucus turnover sloughs it off and release 5-ASA in the upper intestine. Options for final dosage form once microparticles optimized are gastro-resistant or enteric formulations. In this case gamma scintigraphy may be used to investigate the efficiency and operation of the enteric coating and thus, protection from 5-ASA release in the upper regions of the GIT.

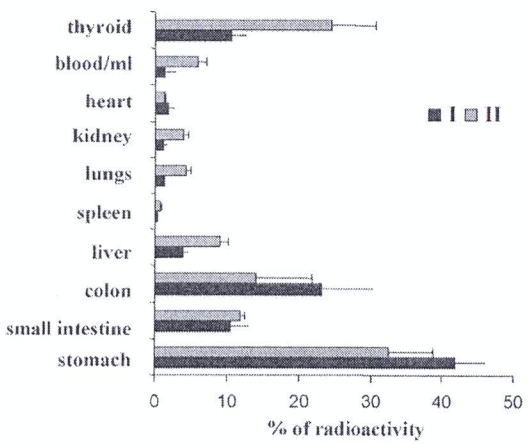


Fig. 13. Biodistribution of [$^{131}$I]-5-ASA loaded chitosan-Ca-alginate microparticles, 24 h after peroral administration to Wistar rats with TNBS induced ulcerative colitis; 5-ASA loaded microparticles (group I) and 5-ASA suspension (group II).

Significantly higher radioactivity detected in the thyroid in the group II after 48 h, as in all periods of the study, supported again the higher amount of systemically absorbed 5-ASA and subsequent iodolysis when as suspension administered (Fig. 14). In this period of the study (48 h), radioactivity in the liver was observed (13.21 ± 3.31%) in the group of rats treated with microparticles (group I), which can be probably explained by the absorption and hepatic metabolism of 5-ASA released from the particles.

## 4. Conclusion

In conclusion, new chitosan-Ca-alginate microparticulated drug delivery system for colon-specific delivery and controlled release of 5-ASA after peroral administration was prepared using spray-drying method followed by ionotropic gelation/polyelectrolyte complexation. Negatively charged particles were obtained with size less than 9 μm. Acceptable spherical morphology was observed, but also flattened disk-shaped particles with smooth surface and low porosity. Chitosan was localized dominantly in the particle wall, while for alginate, a homogeneous distribution throughout the particles was observed. Previous $^{1}$H NMR and FTIR spectra of 5-ASA showed that the formulation and the technology applied ensure 5-ASA stability during microencapsulation and in simulated *in vivo* drug

release conditions when different pH mediums were used. X-ray and DSC studies indicated molecularly dispersed drug within the particles. *In vitro* drug release studies confirmed the potential of the particles to release the drug in a controlled manner. Linear square-root time kinetics of all plots suggests release governed by drug dissolution and diffusion in the aqueous path created in matrix by polymer hydration. The diffusional exponents according to the general exponential release equation indicated anomalous (non-Fickian) transport in 5-ASA release controlled by polymer relaxation, erosion and degradation. Biodistribution studies of $^{131}$I-5-ASA loaded chitosan-Ca-alginate microparticles after peroral administration on Wistar male rats in which TNBS colitis was induced, confirmed the dominant localization of 5-ASA in the colon with low systemic bioavailability.

These data and the studies related to the efficacy of this microparticulate system against colonic inflammation in rats (not presented in this paper) showed that the described system may be useful for clinical treatment of human colonic inflammatory bowel diseases.

## Acknowledgments

This work was supported by a grant from NATO SfP Program; Project No 978023 titled "Influence of biopolymer interactions on the drug delivery from chitosan-alginate colloidal carrier systems". Authors wish to acknowledge Mr. R. Filmon (SCIAM, Angers, France) for his technical assistance in CLSM and SEM imaging.

## References

Acarturk, F., Takka, S., 1999. Calcium alginate microparticles for oral administration. II. Effect of formulation factors on drug release and drug entrapment efficiency. J. Microencapsul. 16, 291–301.

Bantel, H., Berg, C., Vieth, M., Stolte, M., Kruis, W., Schulze-Osthoff, K., 2000. Mesalamine inhibits activation of transcription factor NF-κB in inflamed mucosa of patients with ulcerative colitis. Am. J. Gastroenterol. 95, 3452–3457.

Bernkop-Schnurch, A., Kast, E.C., Richter, F.M., 2001. Improvement in the mucoadhesive properties of alginate by the covalent attachment of cysteine. J. Control. Rel. 71, 277–285.

Bernstein, C.N., Eaden, J., Steinhart, H., Munkholm, P., Gordon, P.H., 2002. Cancer prevention in inflammatory bowel disease and the chemoprophylactic potential of 5-Aminosalicylic acid. Inflam. Bowel. Dis. 8, 356–361, Crohn's 7 Colitis Foundation of America, Inc.

Clemett, D., Markham, A., 2000. Prolonged-release mesalazine: a review of its therapeutic potential in ulcerative colitis and Crohn's disease. Drugs 59, 929–956.

Coppi, G., Iannuccelli, V., Leo, E., Bernabei, M.T., Camoreni, R., 2001. Chitosan-alginate microparticles as aprotein carrier. Drug. Dev. Ind. Pharm. 27, 393–400.

D'Acquisto, F., May, M.J., Ghosh, S., 2002. Inhibition of nuclear factor kappa B (Nf-κB): an emerging theme in anti-inflammatory therapies. Mol. Intervent. 2, 22–35.

De Jaeghere, F., Allemann, R., Doelker, E., Gurny, R., Cerny, R., Galli, B., Steulet, A.F., Muller, I., Schutz, H., 2001. pH-dependent dissolving nano- and microparticles for improved peroral delivery of a highly lipophilic compounds in dogs. AAPS Pharmsci. 3 (1), article 8 (http://www.pharmsci.org/).

Ewe, K., Schwartz, S., Petersen, S., Press, A.C., 1999. Inflammation does not increase intraluminal pH in chronic inflammatory bowel disease. Dig. Dis. Sci. 44, 1434–1439.

Fundueanu, G., Esposito, E., Mihai, D., 1998. Preparation and characterization of Ca-alginate microspheres by a new emulsification method. Int. J. Pharm. 170, 1–21.

Gaserod, O., Smidsrod, O., Skjak-Braek, G., 1998. Microcapsules of alginate-chitosan I. A quantitative study of the interaction between alginate and chitosan. Biomaterials 19, 1815–1825.

Gaserod, O., Sannes, A., Skjak-Braek, G., 1999. Microcapsules of alginate-chitosan II. A study of capsule stability and permeability. Biomaterials 20, 773–783.

George, M., Abraham, E.T., 2006. Polyionic hydrocolloids for the intestinal delivery of protein drugs: Alginate and chitosan—a review. J. Control. Rel. 114, 1–14.

Giunchedi, P., Torre, M.L., Maggi, L., Conti, B., Conte, U., 1996. Cellulose acetate trimetillate ethylcellulose blends for nonsteroidal anti-inflammatory drug (NSAID) microspheres. J Microencapsul. 13, 89–98.

Gombotz, W.R., Wee, S.F., 1998. Protein release from alginate matrices. Adv. Drug. Del. Rev. 31, 267–285.

Hartmann, G., Bidlingmaier, C., Siegmund, B., Albrich, S., Schulze, J., Tschoep, K., Eigler, A., Lehr, H.A., Endres, S., 2000. Specific type IV phopspho-diesterase inhibitor rolipram mitigates experimental colitis in mice. J. Pharmacol. Exp. Ther. 292, 22–30.

He, P., Davis, S.S., Illum, L., 1999. Chitosan microspheres prepared by spray-drying. Int. J. Pharm. 187, 53–65.

Huang, M., Ma, Z., Khor, E., Lim, L.Y., 2002. Uptake of FITC-chitosan nanoparticles by A549 cells. Pharm. Res. 19, 1488–1494.

Jagtap, A.G., Shirke, S.S., Phadke, A.S., 2004. Effect of polyherbal formulation on experimental models of inflammatory bowel disease. J. Ethnopharmacol. 90, 195–204.

Kaiser, G., Yan, F., Polk, D., 1999. Mesalamine blocks tumor necrosis factor growth innibition and nuclear factor κB activation in mouse colonocytes. Gastroenterology 116, 602–609.

Khairou, K.S., Hassan, R.M., 2002. Temperature-dependence of the electrical conductivity for cross-linked mono-and divalent metal-alginate complexes. High Perform. Polym. 14, 93–102.

Krawiscz, J.E., Sharon, P., Stenson, W.F., 1984. Quantitative assay for acute intestinal inflammation based on myeloperoxidase activity. Gastroenterology 87, 1344–1350.

Kuang, J., Wills, J.C., Trowbridge, D.B., Gray, P., Manning, B.M., Eichwald, E.J., Daynes, R.A., Kuwada, S.K., 2002. Nuclear factor κB inhibitors induce adhesion-dependent colon cancer apoptosis: implications for metastasis. Cancer Res. 62, 6870–6878.

Lamprecht, A., Schafer, U., Lehr, C.M., 2000a. Characterization of microcapsules by confocal laser scanning microscopy: structure, capsule wall composition and encapsulation rate. Eur. J. Pharm. Biopharm. 49, 1–9.

Lamprecht, A., Schafer, U., Lehr, C.M., 2000b. Structural analysis of microparticles by confocal laser scanning microscopy. AAPS Pharm. Sci. Tech. 1, article 17.

Lamprecht, A., Ubrich, N., Yamamoto, H., Schafer, U., Takeuchi, H., Maincent, P., Kawashima, Y., Lehr, C.M., 2001a. Biodegradable nanoparticles for targeted drug delivery in treatment of inflammatory bowel disease. J. Pharmacol. Exp. Ther. 299, 775–781.

Lamprecht, A., Schafer, U., Lehr, C.M., 2001b. Size-dependant bioadhesion of micro-and nanoparticulate carriers to the inflamed colonic mucosa. Pharm. Res. 18, 788–793.

Liu, L.-S., Liu, S.-Q., Ng, S.Y., Froix, M., Ohno, T., Heller, J., 1997. Controlled release of interleukin-2 for tumor immunotherapy using alginate/chitosan porous microspheres. J. Control. Rel. 43, 65–74.

Liu, X.D., Yu, W.Y., Zhang, Y., Xue, W.M., Yu, W.T., Xiong, Y., Ma, X.J., Chen, Y., Yuan, Q., 2002. Characterization of structure and diffusion behaviour of Ca-alginate beads prepared with external or internal calcium sources. J. Microencapsul. 19, 775–782.

Loftus, E.V., Kane, S.V., Bjorkman, D., 2004. Systematic review: short-term adverse effects of 5-ASA agents in treatment of ulcerative colitis. Aliment. Pharmacol. Ther. 19, 179–189.

MacDermott, M.D., Richard, P., 2000. Progress in understanding the mechanisms of action of 5-aminosalicylic acid. Am. J. Gastroenterol. 95, 3343–3345.

Mladenovska, K., Janevik, E.I., Glavas, D.M., Kumbaradzi, E.F., Goracinova, K., 2002. Biodistribution studies of BSA loaded gelatin microspheres after peroral application. Int. J. Pharm. 242, 251–253.

Mladenovska, K., Janevik, E.I., Glavas, D.M., Kumbaradzi, E.F., Goracinova, K., 2003. Biodistribution of 131I-BSA loaded gelatin microspheres after peroral application to BALB/c mice—particle size study. Acta Pharm. 53, 187–197.

Morris, G.P., Beck, P.L., Herridge, M.S., Depew, W.T., Scewczuk, M.R., Wallace, J.L., 1989. Hapten-induced model of chronic inflammation and ulceration in the rat colon. Gastroenterology 96, 795–803.

Prakash, A., Markharm, A., 1999. Oral delayed release mesalazine: a review of its therapeutic potential in ulcerative colitis and Crohn's disease. Drugs 57, 383–408.

Ritger, P., Peppas, N.A., 1987. A simple equation for description of solute release II. Fickian and anomalous release from swellable devices. J. Control. Rel. 5, 37–42.

Rodriguez, M., Antunez, J.A., Taboada, C., Seijo, B., Torres, D., 2001. Colon-specific delivery of budenoside from microencapsulated cellulosic cores: evaluation of the efficacy against colonic inflammation in rats. J. Pharm. Pharmacol. 53, 1207–1215.

Rogler, G., Brand, K., Vogl, D., Page, S., Hofmeister, R., Andus, T., Kneuchel, R., Bauerle, P.A., Scholmerich, J., Gross, V., 1998. Nuclear factor κB is activated in macrophages and epithelial cells of inflamed intestinal mucosa. Gastroenterology 115, 357–369.

Sandborn, W.J., Hanauer, S.B., 2003. Systematic review:the pharmacokinetic of oral mesalazine formulations and mesalazine pro-drugs used in the menagement of ulcerative colitis. Aliment. Pharmacol. Ther. 17, 29–42.

Sardar, M., Roy, I., Gupta, M.N., 2003. A smart bioconjugate of alginate and pectinase with unusual biological activity toward chitosan. Biotechnol. Prog. 19, 1654–1658.

Schreiber, S., 1999. Activation of nuclear factor κB as a target for anti-inflammatory therapy. Gut 441, 309–310.

Schreiber, S., Nikolaus, S., Hampe, J., 1998. Activation of nuclear factor κB in inflammatory bowel disease. Gut 42, 477–484.

Shin-ya, Y., Lee, M., Hinode, H., Kajiuchi, T., 2001. Effects of N-acetylating degree on N-acetylated chitosan hydrolysis with commercially available and modified pectinases. Biochem. Eng. J. 7, 85–88.

Takka, S., Acarturk, F., 1999. Calcium alginate microparticles for oral administration. I. Effect of sodium alginate type on drug release and drug entrapment efficiency. J. Microencapsul. 16, 275–290.

Tapia, C., Escobar, Z., Costa, E., Sapag-Hagar, J., Valenzuela, F., Basualto, C., Gai, M.N., Yazdani-Pedram, M., 2004. Comparative studies on polyelectrolyte complex and mixtures of chitosan-carageenan as prolonged diltiazem clorhydrate release systems. Eur. J. Pharm. Biopharm. 57, 65–75.

Tozaki, H., Kamoike, J., Tada, C., Maruyama, T., Terabe, A., Suzuki, T., Yamamoto, A., Muranishi, S., 1997. Chitosan capsules for colon-specific drug delivery: improvement of insulin absorption from the rat colon. J. Pharm. Sci. 86, 1016–1021.

Tozaki, H., Odoriba, T., Okada, N., Fujita, T., Terabe, A., Suzuki, T., Okabe, S., Muranishi, S., Yamamoto, A., 2002. Chitosan capsules for colon-specific drug delivery: enhanced localization of 5-aminosalicylic acid in the large intestine accelerates healing of TNBS-induced colitis in rats. J. Control. Rel. 82, 51–61.

Turkoglu, M., Ugurlu, T., 2002. *In vitro* evaluation of pectin-HPMC compression coated 5-aminosalicylic acid tablets for colonic delivery. Eur. J. Pharm. Biopharm. 53, 65–73.

Ugwoke, M.I., Verbeke, N., Konget, R., 1997. Microencapsulation of apomorphine HCl with gelatin. Int. J. Pharm. 148, 23–32.

Verziji, J.M., van Bodegraven, A.A., 2003. Mesalazine-still a first line therapy. Gastroenterol. Eur. Pharmacother., 29–34.

Wahl, C., Liptay, S., Adler, G., Schmid, R.M., 1998. Sulfasalazine: a potent and specific inhibitor of nuclear factor kappa B. J. Clin. Invest. 5, 1163–1174.

Wittaya-areekul, S., Kruenate, J., Prahsarn, C., 2006. Preparation and in vitro evaluation of mucoadhesive properties of alginate/chitosan microparticles containing prednisolone. Int. J. Pharm. 312, 113–118.

Yue, G., Sun, F.F., Dunn, C., Yin, K., Wong, P.Y., 1996. The 21-aminosteroid tirilazad mesylate can ameliorate inflammatory bowel disease in rats. J. Pharmacol. Exp. Ther. 276, 265–270.

Zambito, Y., Di Colo, G.D., 2003. Preparation and in vitro evaluation of chitosan matrices for colonic controlled drug delivery. J. Pharm. Pharmacol. Sci. 6, 274–281.

Zerrouk, N., Gines Dorado, J.M., Arnaud, P., Chemtob, C., 1998. Physical characteristics of inclusion compounds of 5-ASA in α and β cyclodextrins. Int. J. Pharm. 171, 19–29.

Zhou, S.Y., Fleisher, D., Pao, L.H., Li, C., Winward, B., Zimmermann, E.M., 1999a. Intestinal metabolism and transport of 5-aminosalicylate. Drug. Metabol. Dispos. 27, 479–485.

Zhou, S.Y., Piyapolrungroj, N., Pao, L., Li, C., Liu, G., Zimmermann, E., Fleisher, D., 1999b. Regulation of paracellular absorption of cimetidine and 5-aminosalicylate in rat intestine. Pharm. Res. 16, 1781–1785.